



Palladium Gallium Intermetallic Compounds for the Selective Hydrogenation of Acetylene

Part II: Surface Characterization and Catalytic Performance

J. Osswald¹, K. Kovnir^{1,2}, M. Armbrüster^{1,*}, R. Giedigkeit², R. E. Jentoft¹, U. Wild¹, Y. Grin², R. Schlögl^{1,*}

¹ Department of Inorganic Chemistry, Fritz Haber Institute of the Max Planck Society, Berlin 14195, Germany

² Max-Planck-Institut für Chemische Physik fester Stoffe, Nöthnitzer Str. 40, 01187 Dresden, Germany

* Corresponding author: e-mail research@armbruester.net, Phone:+44(0)1223 33 65 33 Fax:+44(0)1223 33 63 62
current address: University of Cambridge, Chemistry Department, Lensfield Road, Cambridge CB2 1EW UK

Received 21 February 2008; revised 4 June 2008; accepted 13 June 2008. Available online 17 July 2008

Abstract

The structurally well-defined intermetallic compounds PdGa and Pd₃Ga₇ constitute suitable catalysts for the selective hydrogenation of acetylene. The surface properties of PdGa and Pd₃Ga₇ were characterized by X-ray photoelectron spectroscopy, ion scattering spectroscopy and CO chemisorption. Catalytic activity, selectivity and long-term stability of PdGa and Pd₃Ga₇ were investigated under different acetylene hydrogenation reaction conditions, in absence and in excess of ethylene, in temperature-programmed and isothermal long-term experiments. Chemical treatment with ammonia solution – performed to remove the gallium oxide layer introduced during the milling procedure from the surface of the intermetallic compounds – yielded a significant increase in activity. Compared to Pd/Al₂O₃ and Pd₂₀Ag₈₀ reference catalysts, PdGa and Pd₃Ga₇ exhibited a similar activity per surface area, but higher selectivity and stability. The superior catalytic properties are attributed to the isolation of active Pd sites in the crystallographic structure of PdGa and Pd₃Ga₇ according to the active-site isolation concept.

Keywords: palladium, gallium, PdGa, Pd₃Ga₇, acetylene hydrogenation, site isolation, intermetallic compound, X-ray photoelectron spectroscopy, ion scattering spectroscopy, CO chemisorption, chemical etching

1. Introduction

Selective hydrogenation of acetylene ($C_2H_2 + H_2 \rightarrow C_2H_4$, $\Delta H = -172$ kJ/mol) is an important industrial process to remove traces of acetylene in the ethylene feed for the production of polyethylene. Because acetylene poisons the catalyst for the polymerization of ethylene to polyethylene, the acetylene content in the ethylene feed has to be reduced to the low ppm range [1-3]. Moreover, economic efficiency requires high selectivity of the acetylene hydrogenation in the presence of an excess of ethylene to prevent the hydrogenation of ethylene to ethane. Typical hydrogenation catalysts contain palladium dispersed on metal oxides. While palladium metal exhibits high activity, it possesses only limited selectivity and long-term stability because of the formation of ethane by total hydrogenation as well as C4

species and higher hydrocarbons by oligomerisation reactions [4-5].

Modification of palladium catalysts by adding promoters or alloying with other metals has been shown to result in an increased selectivity and long-term stability in the hydrogenation of acetylene [6-7]. However, the catalytic performance of these modified Pd catalysts remains insufficient and further improvements in selectivity may decrease the costs for the production of polyethylene. In addition to unsatisfactory selectivity, the long-term stability of palladium catalysts has to be improved. Catalyst deactivation by carbonaceous deposits requires frequent exchange or regeneration of the catalyst in the hydrogenation reactor. Moreover, fresh or regenerated catalysts show high activity and local overheating (“thermal run away”) of the reactor and, consequently, lead to increased ethylene consumption and loss in selectivity.

The limited selectivity of Pd catalysts in acetylene hydrogenation can be attributed to the presence of active-site ensembles on the catalyst surface [6, 8-9]. Active-site isolation increases Pd-Pd distances on the catalyst surface and may lead to only weakly π -bonded acetylene on top of an isolated Pd atom. Furthermore, the sequential hydrogenation of acetylene to ethylene via vinyl and vinylidene intermediates requires a decreasing active site size [10]. Therefore, a reduction of neighbouring palladium sites on the surface should yield preferred hydrogenation of acetylene to ethylene [2, 11-17].

In the intermetallic compounds PdGa [18-20] and Pd₃Ga₇ [20-22] the Pd atoms are only surrounded by gallium atoms in the first coordination shell and, thus, may be promising catalysts with an improved selectivity and long-term stability in acetylene hydrogenation [23]. Furthermore, modification of the electronic structure by promoting or alloying of the Pd catalyst to tailor adsorption or desorption properties may be employed to increase the selectivity in hydrogenations [6]. In addition to the local structure around the active Pd sites compared to Pd metal or conventional Pd alloys, Pd-Ga intermetallic compounds exhibit a modified electronic structure which may further improve their catalytic performance in acetylene hydrogenation [10].

Part I of this work describes the preparation of the Pd-Ga intermetallic compounds PdGa and Pd₃Ga₇ and elucidates their thermal and structural stability under various reaction conditions [24]. Part II presents results of the surface characterization by X-ray photoelectron spectroscopy, ion scattering spectroscopy and CO chemisorption measurements. The catalytic performance of PdGa and Pd₃Ga₇ in acetylene hydrogenation was investigated and compared to Pd/Al₂O₃ and an unsupported palladium-silver alloy.

2. Experimental

2.1. Synthesis and Materials

Details of the preparation of the Pd-Ga intermetallic compounds are described in Part I [24]. The alloy referred to as Pd₂₀Ag₈₀ in the following, was prepared by melting together 1.2047 g Ag (99.995% ChemPur) and 0.3035 g Pd (99.95% ChemPur) three times in an arc melter under argon. Subsequently, the regulus obtained was enclosed in an evacuated quartz glass ampoule and annealed at 800 °C for six days. After the heat treatment, the regulus was filed and the phase purity of the obtained Pd-Ag alloy (Cu type of structure, $Fm\bar{3}m$, $a = 4.0456(6)$ Å) was confirmed by X-ray powder diffraction (STOE STADI P diffractometer, Cu K α_1 radiation, $\lambda = 1.540598$ Å, curved Ge monochromator).

2.2. Chemical Etching

To increase the active catalyst surface, chemical etching was performed using ammonia solution at various pH-values. Commercial ammonia solution (Merck, 25%, p.a.) was diluted with distilled water to the required pH-value. pH measurements were performed with a Knick pH-Meter 761 Calimatic and a Mettler-Toledo Inlab 422 electrode calibrated with buffer solutions (Merck centiPUR pH = 7 and pH = 9). Usually, 30 to 50 mg PdGa or Pd₃Ga₇ were added to 75 ml of the ammonia solution and stirred for 10 minutes at 300 K. The solution was filtered and the powder was washed with additional 50 ml of the ammonia solution. Etched samples were dried for 120 min in a desiccator evacuated to 10 mbar and stored under Ar in a glove box.

2.3. XPS and ISS

X-ray photoelectron spectroscopy (XPS) and ion scattering spectroscopy (ISS) were performed with a Leybold LHS 12 MCD UHV system. The samples for the measurements were prepared from milled PdGa and Pd₃Ga₇ powder. XPS data were obtained using Al K α radiation (1486.6 eV) and a pass energy of 48 eV resulting in a spectrometer resolution of 1.1 eV. Shirley background correction and numeric integration of the peak areas were employed for XPS data reduction. Elemental composition of the near-surface region was estimated from the peak areas obtained using the corresponding sensitivity factors [25]. The palladium content was calculated from a sum of the Pd3d_{3/2} and Pd3d_{5/2} peaks and the carbon content was obtained from the C1s peak. Because of the overlapping O1s and Pd3p_{3/2} peaks in the XP spectra, the Pd3p_{3/2} peak area was calculated from the Pd3d_{3/2} and Pd3d_{5/2} peak areas assuming a factor of 2.9 for the (Pd3d_{3/2} + Pd3d_{5/2})/Pd3p_{3/2} ratio [25]. Subsequently, the Pd3p_{3/2} peak area obtained was subtracted from the O1s peak area to calculate the oxygen content in the near-surface region. The determined values possess a relative error of 10%. The amounts of gallium and gallium oxide were determined by fitting the Ga2p_{3/2} peak with two Gauss-Lorentz profile functions (30% Lorentzian). Due to the overlapping signals, the relative error of the concentration is in the region of 20-30%. All XPS spectra were corrected for charging effects by setting the binding energy of the C1s peak to 284.6 eV [26].

Ion scattering spectroscopy was performed using He ions with a kinetic energy of 2 keV and an emission current of 10 mA resulting in an ion current of 1.65 μ A at the sample. For ISS measurements of PdGa the first two scans were averaged and the following scans were averaged in groups of ten. In the case of Pd₃Ga₇, the first three scans were averaged and the following scans were averaged in groups of ten. Milled samples of PdGa and Pd₃Ga₇ were measured first by XPS followed by ISS measurements and

another XPS measurement to reveal the surface composition of the materials and the influence of the ion scattering thereon. The influence of a hydrogen treatment on the surface composition was determined by XPS measurements before and after reduction of milled PdGa in 200 mbar H₂ at 573 K for 30 min. After a second hydrogen treatment at 673 K for 30 min, XPS spectra were taken again followed by ISS and XPS measurements. Because of the reduced thermal stability of Pd₃Ga₇, XPS and ISS measurement were performed before and after a single hydrogen treatment at 573 K according to the procedure described above.

2.4. CO Chemisorption

Carbon monoxide chemisorption measurements were carried out in an Autosorb 1C (Quantachrome Instruments). The samples (PdGa: 1.5 g, Pd₃Ga₇: 1 g, Pd/Al₂O₃: 180 mg) were pre-treated in the sample cell by heating them to different reduction temperatures – 673 K (Pd₃Ga₇), 773 K (PdGa) or 473 K (Pd/Al₂O₃) in helium flow (20 ml/min), followed by an isothermal hydrogen treatment for 30 min (20 ml/min of hydrogen flow) and evacuation (180 min) at the pretreatment temperature. The samples were cooled down to 300 K under vacuum and additionally evacuated for 180 min. Subsequently, the CO chemisorption measurements (CO 4.7, Westfalen Gas, Germany) were performed at 300 K.

The active Pd surface area was determined by stepwise measuring the amount of chemisorbed and physisorbed CO. An initial CO pressure of 10.7 kPa was employed, followed by nine equidistant steps up to a final pressure of 106.7 kPa. The pressure drop in the sample cell can be used to calculate the amount of CO adsorbed. Both the extrapolation method and the dual isotherm method were used to distinguish between chemisorbed and physisorbed CO and to determine the active-surface area. A stoichiometric factor of 1.5 was used to account for the presence of on-top and bridged bond CO molecules on the Pd surface [27-28]. Further details are given elsewhere [29-32].

2.5. Catalysis Measurements

Catalytic investigations were performed in a plug flow reactor consisting of a quartz glass tube with a length of 300 mm, an inside diameter of 7 mm and a sintered glass frit to support the catalyst. For temperature control, a thermocouple was placed inside the catalyst bed. The reactant gases were mixed with Bronkhorst mass flow controllers to a total flow of 30 ml/min. A Varian CP 4900 micro gas chromatograph (GC) and a Pfeiffer Omnistar quadropol mass spectrometer (MS) were used for effluent gas analysis. The Varian MicroGC contained four modules, each with an individual column and a thermal conductivity detector. Hydrogen and helium from the feed gas, and possible oxygen and nitrogen impurities because of leaks in the

set-up, were separated on a molsieve column. Acetylene, ethylene and ethane were separated on an alumina column. The total concentration of C4 hydrocarbons (1-butene, 1,3-butadiene, n-butane, trans- and cis-2-butene) was determined using a dimethylpolysiloxane column. Higher hydrocarbons were also separated on the siloxan column but not further quantified because of the presence of many different C6 and C8 hydrocarbons and their low total concentration (less than 0.1% of absolute product stream concentration). Argon (6.0) and helium (6.0) were used as carrier gases for the molsieve column and for the other columns, respectively. A measurement cycle including stabilization, sampling, injection and separation took between 4 and 5 minutes.

Acetylene hydrogenation experiments were carried out under two different reactive gas atmospheres: gas composition A (2% acetylene and 4% hydrogen in helium) and gas composition B (0.5% acetylene, 5% hydrogen and 50% ethylene in helium). Solvent free acetylene (2.6), hydrogen (5.0) and helium (5.0) were used for studies under gas composition A, while a mixture of 2% acetylene in helium (C₂H₂: 2.6, He: 4.6), hydrogen (5.0), ethylene (3.5) and helium (5.0) was used for studies under gas composition B. The solvent free acetylene was obtained from Linde (Germany), while all other gases were obtained from Westfalen Gas (Germany).

Activity and selectivity of the materials in the hydrogenation of acetylene were measured by temperature-programmed as well as by isothermal experiments. In the temperature programmed mode, the composition of the product gas stream was measured every 15 K, after stabilizing the catalysts for 15 min, in the range from 298 K to 613 K (gas composition A). In the isothermal mode, the experiments were performed at 393 K (gas composition A) and 473 K (gas composition B). The conversion *Conv* was calculated using the following equation:

$$Conv = \frac{C_{feed} - C_x}{C_{feed}}$$

where *C_x* is the acetylene concentration in the product stream and *C_{feed}* is the acetylene concentration in the feed before the reaction. With the gas composition A, the selectivity *Sel_A* is calculated according to

$$Sel_A = \frac{C_{ethylene}}{C_{ethylene} + C_{ethane} + 2C_{C_4H_x}}$$

where *C_{C₄H_x}* is the sum of the C4 hydrocarbons. The change in ethylene concentration Δ*C_{ethylene}* cannot be accurately measured in an excess of ethylene (gas composition B) and, hence, cannot be used for calculating the selectivity. Therefore, the selectivity *Sel_B* was calculated from the following equation, with *C_{feed}* as the acetylene concentration before and *C_x* as the acetylene concentration after the reactor:

$$Sel_B = \frac{C_{feed} - C_x}{C_{feed} - C_x + C_{ethane} + 2C_{C_4H_x}}$$

Calculation of the selectivity with gas composition B assumes that acetylene is only hydrogenated to ethylene, which may be further hydrogenated to ethane. The amount of higher hydrocarbons and carbon deposits formed was assumed to be negligible. In addition to hydrogenation of acetylene to ethane, ethylene from the feed may be hydrogenated to ethane, which is included in the selectivity equation. To measure the selectivity at the same conversion for different catalysts, the used amounts were adjusted according to the specific activity of the catalysts as determined in previous experiments. The activity Act of the samples was calculated using the following equation:

$$Act = \frac{Conv \cdot C_{feed} \cdot C_{exp}}{m_{cat}}$$

where m_{cat} is the amount of used catalyst in g and the constant C_{exp} is 1.904 g/h. The constant was introduced to convert the acetylene flow from [ml/min] units to [g/h], is based on the perfect gas model

$$C_{exp} = \frac{M_{acet} \cdot p \cdot F}{R \cdot T}$$

where M_{acet} is the molecular weight of acetylene (26 g/mol), p the pressure (1.013 bar) and F the total gas flow through the reactor at room temperature (1.8 l/h at 300 K). R is the universal gas constant (8.3144 J/(molK)) and T the temperature (300 K).

To improve the flow characteristics the corresponding amount of unsupported sample was diluted with 30 mg (gas composition A) or 50 mg (gas composition B) inactive boron nitride (hexagonal, 99.5%, 325 mesh, Aldrich). A commercial Pd/Al₂O₃ catalyst (5 wt.-% Pd, Aldrich) was used as reference in both gas compositions. Additionally, an unsupported palladium silver alloy Pd₂₀Ag₈₀ was used as benchmark catalyst for studies with gas composition B.

3. Results and Discussion

3.1. Surface Characterization of PdGa and Pd₃Ga₇

In the bulk structures of PdGa and Pd₃Ga₇ palladium atoms exclusively possess gallium atoms as nearest neighbors. Furthermore, the compounds exhibit a pronounced stability under hydrogenation reaction conditions as determined by *in situ* DSC/TG, *in situ* XRD and *in situ* EXAFS investigations [10, 24]. From the stoichiometry of PdGa and Pd₃Ga₇, an average surface composition of 50% gallium and 50% palladium, and 70% gallium and 30% palladium, respectively, may be assumed. Because the real composition and the structure of the surface of these materials may differ from those of the bulk, the milled and pre-treated Pd-Ga intermetallic compounds were further characterized by various surface sensitive techniques.

XPS data of PdGa revealed that the near-surface region of milled but unetched material mainly consists of

Table 1: Surface composition retrieved from XPS data (at%) of milled PdGa, after hydrogen treatment at 573 and 673 K as well as after ISS measurements

PdGa	Ga2p _{3/2}	O1s	Cl1s	Pd3d
Untreated	32	57	5	6
H ₂ treatment at 573 K	39	49	7	7
H ₂ treatment at 673 K	37	47	6	10
After ISS	40	41	2	17

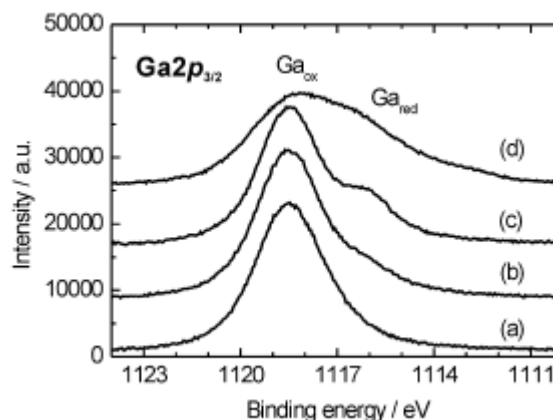


Figure 1: XPS data of the Ga_{2p_{3/2}} peak of milled PdGa (a) untreated, (b) after H₂ treatment at 573 K, (c) after H₂ treatment at 673 K, and (d) after ISS. The shoulder at lower binding energy represents a reduced Ga species.

oxygen and gallium (Table 1 and Fig. 1), while the concentration of palladium amounted to only 6%. After hydrogen treatment at 573 K and 673 K for 30 minutes, the oxygen content decreased from 57% to 49% and 47%, respectively. The palladium concentration in the near-surface region increased to 10% after hydrogen treatment at 673 K and reached 17% after the ISS measurements. The XPS data of air milled PdGa exhibited only a broad Ga_{2p_{3/2}} peak at 1118.5 eV indicating that only gallium oxide is present on the surface [33]. The reduced gallium species on the surface of the milled PdGa intermetallic compound seems not to be detectable by XPS under the conditions employed. After hydrogen treatment at 573 K and 673 K, a shoulder of the Ga_{2p_{3/2}} peak at lower binding energy was observed indicative of the formation of a reduced gallium species (Figure 1). After ion sputtering during the ISS measurements, a very broad (FWHM > 4 eV) Ga_{2p_{3/2}} peak appeared representing a mixture of metallic and oxidized gallium. Curve fitting of the Ga_{2p_{3/2}} peak resulted in an increased metallic gallium content. However, 74% of the gallium remains in an oxidized state after hydrogen treatment at 673 K (Table 2). The Ga_{2p_{3/2}} peak measured after hydrogen treatment at 673 K exhibited a binding energy of 1116.7 eV, which is in good agreement with the value for metallic gallium (1116.3 eV [33]). The Pd_{3d_{5/2}} peak of PdGa after hydrogen treatment at 673 K was located at a binding energy of 335.7 eV similar to previously reported values for as-prepared PdGa (336.0 eV) [10,34].

XPS data of milled Pd₃Ga₇ showed a similar oxygen content of the near-surface region as PdGa. In contrast to PdGa, the amount of oxygen was not significantly reduced after thermal treatment in hydrogen. The palladium content of the surface was very low and remained at 2% after hydrogen treatment at 573 K. Only after He ion sputtering during ISS measurements, the oxygen content was reduced

Table 2: Amount of oxidized and metallic Ga at the surface of milled PdGa and Pd₃Ga₇, and after H₂ treatment calculated from Ga₂p_{3/2} XPS peak refinement (at%)

Treatment	PdGa		Pd ₃ Ga ₇	
	Oxidized	Metallic	Oxidized	Metallic
Untreated	94	6	96	4
H ₂ treatment at 573 K	84	16	97	3
H ₂ treatment at 673 K	74	26	-	-

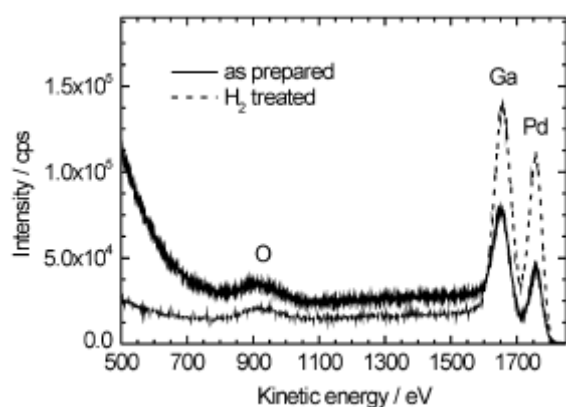


Figure 2: ISS data of milled but chemically unetched PdGa (averaged first two scans) and after additional H₂ treatment at 673 K. Peaks at 1750 eV (Pd), 1650 eV (Ga) and 910 eV (O) are indicated.

to 36% and the gallium and palladium content increased to 51% and 11%, respectively. XPS data of milled Pd₃Ga₇ exhibited one broad Ga₂p_{3/2} peak indicating that only gallium oxide was detected on the surface. While the width of the Ga₂p_{3/2} peak decreased after hydrogen treatment at 573 K, no additional shoulder was observed (Table 2). Only after He ion sputtering, two Ga₂p_{3/2} peaks were obtained, revealing a mixture of metallic gallium and gallium oxide in the near-surface region.

The observed gallium oxide layer indicates a segregation of gallium to the surface of PdGa and Pd₃Ga₇ followed by oxidation to gallium oxide. Since all syntheses were performed in an argon-filled glovebox with moisture and oxygen levels less than 1 ppm the surface mostly oxidized during the milling of the samples in air. After reductive treatment at elevated temperatures, no segregation of Pd atoms to the surface of the Pd-Ga intermetallic compounds and no formation of Pd clusters or overlayers was detected. Hence, the structural stability as determined by *in situ* XRD and EXAFS does also hold for the near-surface region of the intermetallic compounds used [24].

In contrast to XPS which reveals the composition of the near-surface region within a few nanometers, ISS is more surface sensitive and yields the composition of the top most surface layer. During ISS measurements the surface layers will be removed by He ions, leading to a depth profiling of the material studied. ISS spectra (first 2 scans) of untreated PdGa and of PdGa after hydrogen treatment at 673 K are depicted in Figure 2. The kinetic energy of the scattered He ions depends on the energy of the incident beam, the incident angle and the mass of the scattering atoms on the surface of the material studied [26]. Because scattering at heavier elements results in He ions with higher kinetic energy, the peak in the ISS spectra at the highest kinetic energy can be assigned to Pd atoms on the surface. An ISS peak at a kinetic energy of 1650 eV corresponds to Ga atoms, while light elements like carbon and oxygen scatter He ions with kinetic energy in the range from 800 to 1000 eV.

After hydrogen treatment at 673 K the Pd/Ga peak ratio increased from 0.59 to 0.77 (Figure 2). Because the total cross-sections of the various elements in ISS depend on various unknown factors, the elemental composition of the surface region cannot be accurately quantified from the ISS data taken. Assuming a stoichiometric composition (1:1) of both the surface and the bulk of PdGa, the amplitude of the Pd peak should be higher than the corresponding Ga amplitude. Conversely, the ISS spectra indicate an excess of gallium on the surface in agreement with the XPS data, thus clearly excluding the segregation of palladium to the surface. While the amplitude of the oxygen ISS peak was reduced after the hydrogen treatment of PdGa, a high concentration of oxygen persisted on the surface. A series of ISS scans of untreated PdGa resulted in different spectra compared to those of hydrogen treated PdGa. After eight series of ISS scans, the Pd peak was higher than the Ga peak and the amount of oxygen on the surface was significantly reduced.

ISS measurement of Pd₃Ga₇ revealed similar results compared to PdGa. Hydrogen treatment at 573 K resulted in a slightly decreased oxygen peak and an increased Ga peak. No change in the Pd peak was observed. A series of ISS measurements resulted in an increasing amount of Ga and Pd on the surface while the amount of oxygen decreased. However, the estimated amount of Pd on the surface remained low compared to the expected composition of Pd₃Ga₇.

The fact that Pd is detectable by ISS excludes a total coverage of the surface of PdGa and Pd₃Ga₇ by the gallium oxide layer. Since the Pd:Ga ratio is lower than 1:1, no segregation of Pd or Pd overlayers were detected in agreement with the XPS data. XPS and ISS experiments showed that sputtering with He atoms removes the gallium oxide layer more efficiently than reduction with hydrogen. However, the gallium oxide that covers the surface of the milled in air Pd-Ga intermetallic compounds will mostly remain under hydrogenation conditions.

To characterize the active Pd surface, CO chemisorption measurements were conducted. Prior to the measure-

ments, PdGa and Pd₃Ga₇ were reduced in hydrogen in the temperature range from 323 K to 773 K and 673 K, respectively. Carbon monoxide adsorption experiments at 300 K showed no chemisorption of CO on the surface of reduced PdGa and Pd₃Ga₇. On the other hand, CO chemisorption measurements of Pd/Al₂O₃ at 300 K resulted in an active Pd surface area of 5.6 m²/g and a metal dispersion of 26%. A detection limit of 0.02 m² Pd metal surface area was estimated for the sorption equipment used.

Because CO chemisorbs strongly on Pd metal surfaces [35], the presence of regular metallic Pd at the surface of the Pd-Ga intermetallic compounds can be excluded, in good agreement with the XPS and ISS measurements. Furthermore, CO adsorbs strongest in the fcc position on Pd(111). Adsorption on top of the Pd atom is energetically less favoured by 0.5 eV [36]. PdGa and Pd₃Ga₇ do not show the structural motif of a threefold Pd site, thus, the energy barrier for the on top adsorption of CO may be the reason, why CO is not adsorbed at 300 K.

The surface characterization of PdGa and Pd₃Ga₇ by XPS, ISS and CO chemisorption revealed a partial Ga₂O₃ coverage which can not be removed completely by hydrogen treatment at elevated temperatures. Ga₂O₃ originates from segregation and oxidation of Ga during the milling process, resulting in a lower than expected Pd:Ga ratio on the surface. According to CO chemisorption measurements the presence of elemental Pd on the surface can be ruled out. Since the temperatures employed for the hydrogen treatment of PdGa and Pd₃Ga₇ were higher here than in the catalytic investigation with gas composition B (see below) the surface composition should be alike under the reaction conditions employed.

3.2. Chemical Etching of Pd-Ga Intermetallic Compounds

To increase the active Pd surface area the Ga₂O₃ surface layer on the intermetallic compounds was removed by chemical etching. Ammonia solution is well-known for chemical etching of semiconductors like GaAs [37-39]. Chemical etching, however, may result in the formation of neighboring Pd atoms and, thus, Pd clusters or Pd overlayers by dissolution of Ga from the bulk structure of the Pd-Ga intermetallic compounds. The latter will cause a significant loss in selectivity of the corresponding catalyst under acetylene hydrogenation conditions and an increased formation of ethane. Therefore, maintaining selectivity while increasing hydrogenation activity of an etched material requires an optimized etching procedure.

PdGa and Pd₃Ga₇ could be successfully chemically etched to obtain a higher activity at nearly the originally high selectivity (see below). The lower pH value required for a successful etching of PdGa (pH 9.8) compared to Pd₃Ga₇ (pH 10.5) indicates a facilitated dissolution of gallium oxide from the surface of PdGa. This may be caused by a reduced interaction at the interface between gallium oxide and PdGa, a more amorphous structure of the gallium

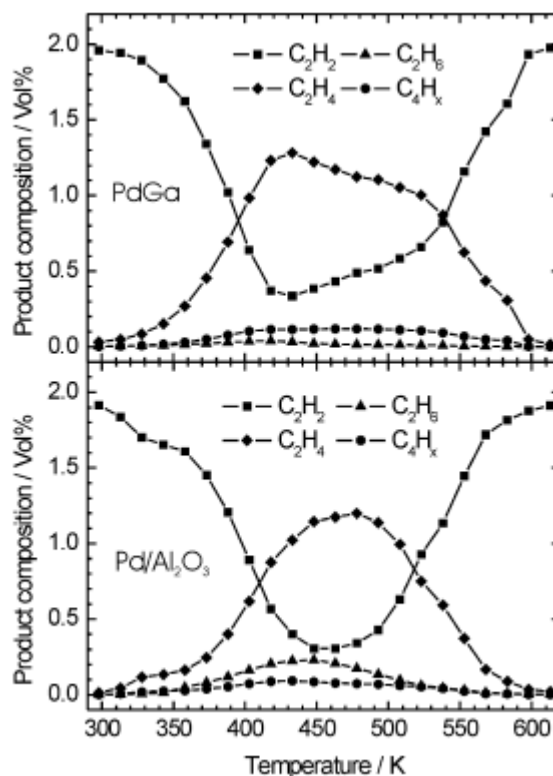


Figure 3: Product composition during hydrogenation of acetylene (2% C₂H₂ + 4% H₂ in helium, gas composition A) on 50 mg PdGa (top) and 0.5 mg Pd/Al₂O₃ (bottom).

oxide or a thinner layer of Ga₂O₃ on PdGa. Using a higher pH for the etching solution resulted in a further increase in activity but a decreased selectivity and enhanced ethane formation. Similarly, an etching solution with an even lower pH of 9.0 had to be employed to maintain high selectivity of the etched catalysts with gas composition B.

The varying influence of the pH of the ammonia solution used on the selectivity of the etched Pd-Ga intermetallic compounds indicates that ammonia solution is not the most suitable agent to selectively remove the gallium oxide layer without structural degradation of the underlying intermetallic compound. Hence, further investigations will have to focus on more selective chemical etching procedures that permit to fully explore the superior catalytic properties of Pd-Ga intermetallic compounds [40].

3.3. Acetylene Hydrogenation (Gas Composition A)

Unetched PdGa showed high activity in acetylene hydrogenation with gas composition A (2% acetylene and 4% hydrogen) (Figure 3) in the range of 370 to 570 K with a maximum at 430 K and an activity of 0.639 g/(g_{cat}h). Chemically untreated Pd₃Ga₇ also showed high activity in the temperature range from 390 K to 570 K with a maximum of 0.313 g/(g_{cat}h) at 490 K. Under these conditions

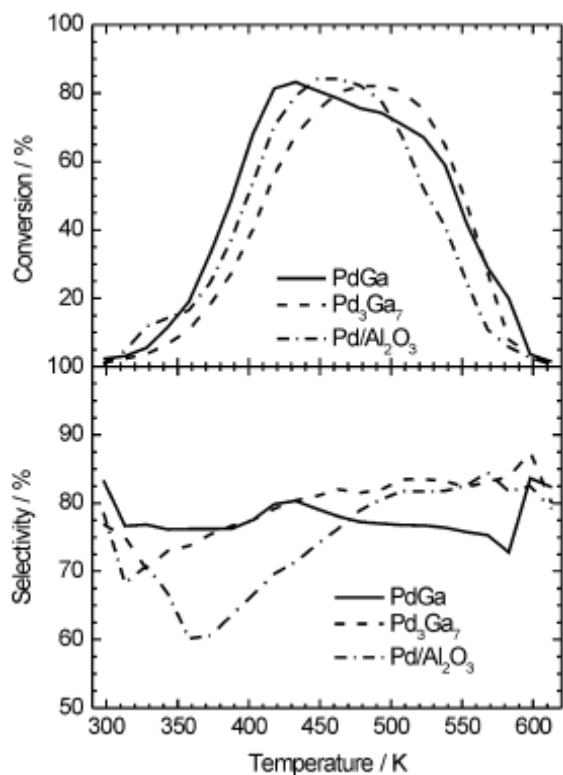


Figure 4: Conversion (top) and selectivity (bottom) during acetylene hydrogenation (temperature dependent, gas composition A) on PdGa (50 mg), Pd₃Ga₇ (100 mg) and Pd/Al₂O₃ (0.5 mg).

more C₄ hydrocarbons than ethane were obtained as by-products. In contrast, acetylene hydrogenation on Pd/Al₂O₃ (activity at 450 K: 64.07 g/(g_{cat}h)) resulted in more ethane than C₄ hydrocarbon formation (Figure 3). Figure 4 shows the acetylene conversion of 50 mg PdGa, 100 mg Pd₃Ga₇ and 0.5 mg Pd/Al₂O₃. The conversion rapidly increased with increasing temperature in the sequence PdGa, Pd/Al₂O₃ and Pd₃Ga₇ and all three catalysts reached a conversion level of 80%. Above 500 K the acetylene conversion of Pd/Al₂O₃ decreased faster than that of the intermetallic compounds. Moreover, Figure 4 depicts a significantly higher selectivity to ethylene in the temperature range from 330 K to 470 K for the Pd-Ga intermetallic compounds compared to Pd/Al₂O₃. At temperatures above 470 K the selectivity of Pd₃Ga₇ is similar to that of Pd/Al₂O₃ and higher compared to that of PdGa.

Acetylene hydrogenation on PdGa and Pd/Al₂O₃ with gas composition A was measured isothermally at 393 K in acetylene feed for 17 hours (Figure 5) to investigate the deactivation behavior of PdGa and Pd/Al₂O₃. In the first two hours, PdGa showed a deactivation from 55% to 45% acetylene conversion followed by a slow increase to about 50% acetylene conversion and an activity of 0.378 g/(g_{cat}h) (Figure 5). The selectivity of PdGa remained constant at 80%, while Pd/Al₂O₃ exhibited a pronounced deactivation behavior during the first two hours from about 95% to 30% conversion. Further deactivation resulted in only 15% acetylene conversion and an activity of 10.81 g/(g_{cat}h) after

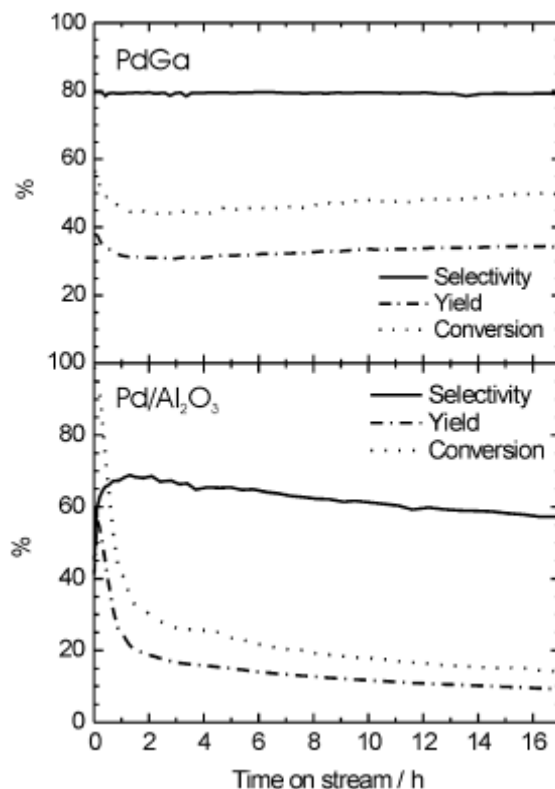


Figure 5: Acetylene conversion and ethylene selectivity of 50 mg PdGa (top) and 0.5 mg Pd/Al₂O₃ (bottom) in acetylene hydrogenation (isothermal at 393 K under gas composition A).

17 hours time on stream. The selectivity of Pd/Al₂O₃ in acetylene hydrogenation to ethylene exhibited a maximum of 70% after two hours and slowly decreased to 55% after 24 hours time on stream.

Chemical etching of PdGa using an ammonia solution at pH = 9.8 resulted in a ten times higher activity (6.860 g/(g_{cat}h) at 450 K) in acetylene hydrogenation while maintaining the high selectivity (Figure 6). Acetylene conversion and selectivity of PdGa depended strongly on the etching conditions used. Increasing the pH to 10 or higher resulted in a further increase in activity, which was accompanied by a strong loss in selectivity. Catalytic performance of Pd₃Ga₇ in acetylene hydrogenation was less dependent on varying the pH of the ammonia solution. The highest activity – keeping relatively high selectivity of Pd₃Ga₇ – was obtained at a pH of 10.5. The maximum in acetylene conversion as a function of temperature was shifted by 40 K to lower temperatures and only 15 mg of chemically etched Pd₃Ga₇ sufficed to reach 80% conversion of acetylene and resulted in nearly seven times higher activity (2.092 g/(g_{cat}h) at 450 K) compared to untreated Pd₃Ga₇. The chemically etched Pd₃Ga₇ sample maintained a similar high selectivity as untreated Pd₃Ga₇.

Untreated Pd-Ga intermetallic compounds showed a low activity compared to Pd/Al₂O₃. After chemical etching (pH = 9.8 for PdGa, pH = 10.5 for Pd₃Ga₇) the activity with gas composition A (2% acetylene and 4% hydrogen) was

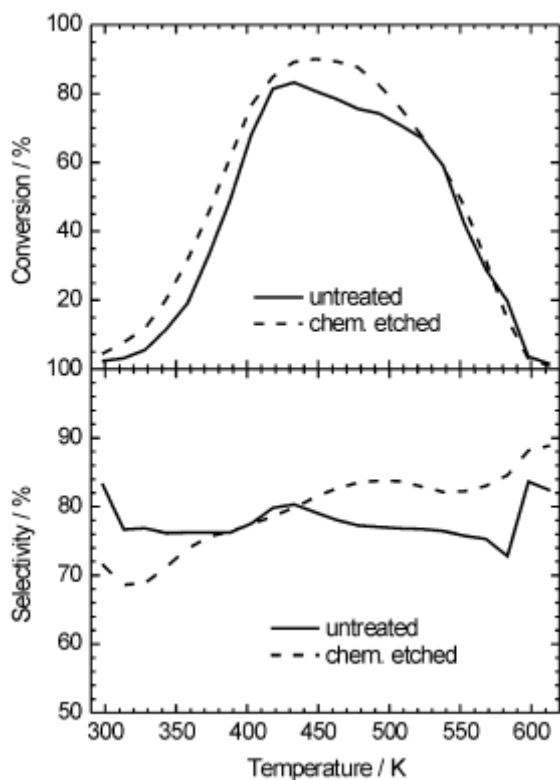


Figure 6: Catalytic performance of untreated (50 mg) and chemically etched (5 mg, pH 9.8) PdGa in acetylene hydrogenation with gas composition A.

improved by 6.7 times for Pd₃Ga₇ and by 10 times for PdGa. In total, activation of milled PdGa and Pd₃Ga₇ in hydrogen is clearly inferior to chemical etching in increasing the active Pd surface area.

3.4. Acetylene Hydrogenation in an Ethylene-Rich Feed (Gas Composition B)

Activity, selectivity and long-term stability of untreated and chemically etched Pd-Ga intermetallic compounds in acetylene hydrogenation were determined in an excess of ethylene with gas composition B (0.5% C₂H₂ + 5% H₂ + 50% C₂H₄ in helium) and compared to the catalytic performance of Pd/Al₂O₃ and the unsupported Pd₂₀Ag₈₀ alloy. First, isothermal catalysis experiments were performed by heating the untreated intermetallic compounds and the reference materials (PdGa: 40 mg, Pd₃Ga₇: 100 mg, Pd/Al₂O₃: 0.15 mg and Pd₂₀Ag₈₀: 200 mg) in helium to a reaction temperature of 473 K followed by switching to the ethylene-rich feed. The acetylene conversion and the corresponding selectivity obtained are plotted in Figure 7. During 20 hours time on stream Pd₃Ga₇ showed a constant acetylene conversion of 99%. PdGa reached a constant acetylene conversion of about 90% after two hours time on stream. Pd₂₀Ag₈₀ showed a nearly constant conversion level of 85%, whereas Pd/Al₂O₃ exhibited

a strong deactivation from 100% to 40% conversion during 20 hours (Figure 7 + Table 3). In addition to a high conversion of acetylene, the untreated intermetallic compounds PdGa and Pd₃Ga₇ possessed a high and long-term stable selectivity of about 70% (Figure 7, Table 3) compared to 50% selectivity of Pd₂₀Ag₈₀ and only 20% selectivity of Pd/Al₂O₃.

Isothermal catalysis experiments were performed by heating the chemically etched intermetallic compounds in helium to a reaction temperature of 473 K followed by switching to the ethylene-rich feed (gas composition B). Generally, the same tendencies were observed as for gas composition A: an increase of the pH-value leads to increasing activity and decreasing selectivity and long-term stability (Fig. 8). Detailed investigations of the etching

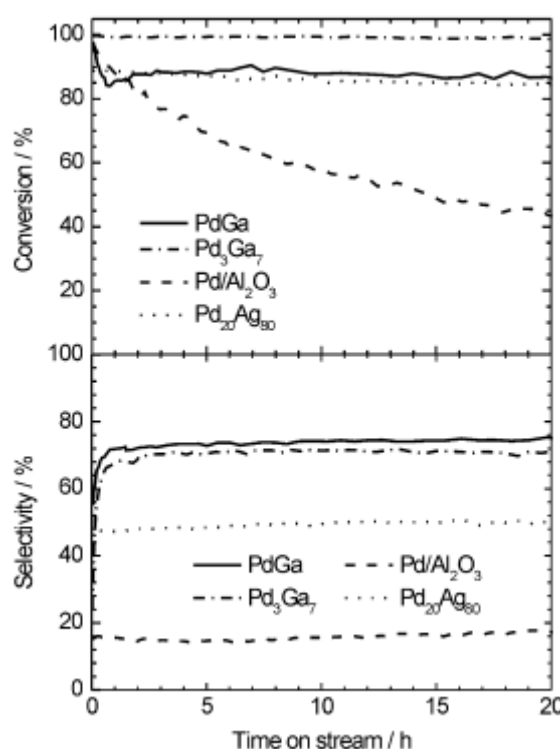


Figure 7: Conversion (top) and selectivity (bottom) of PdGa (40 mg), Pd₃Ga₇ (100 mg), Pd/Al₂O₃ (0.15 mg) and Pd₂₀Ag₈₀ (200 mg) in acetylene hydrogenation (isothermal at 473 K with gas composition B).

Table 3: Acetylene conversion and selectivity of PdGa and Pd₃Ga₇ samples milled in air, as well as of the reference catalysts Pd/Al₂O₃ and Pd₂₀Ag₈₀ after 20 h in an excess of ethylene (gas composition B) at 473 K

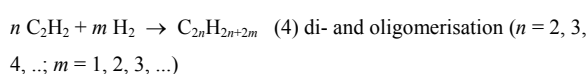
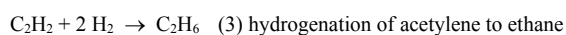
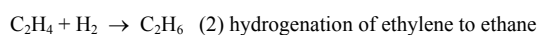
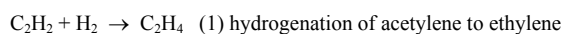
Sample	Sample mass (mg)	Surface area (m ² /g)	Conversion (%)	Selectivity (%)	Activity (g/(g _{cat} h))	Surface activity (g/(m ² _{cat} h))
PdGa	40.0	0.41	86	75	0.205	0.50
PdGa etched (pH 9.8)	1.5	1.0	91	56	5.78	5.78
Pd ₃ Ga ₇	100	0.37	99	71	0.094	0.25
Pd ₃ Ga ₇ etched (pH 10.5)	1.0	2.2	65	48	6.19	2.81
Pd/Al ₂ O ₃	0.15	5.6	43	17	27.29	4.87
Pd ₂₀ Ag ₈₀	200	<0.5	83	49	0.040	0.24*

mechanism, like dissolving of surface gallium oxides and/or dissolving bulk gallium from the intermetallic compounds, by BET, SEM, EDX, XPS and chemical analysis will be published elsewhere [40-41].

With gas composition B (excess of ethylene) the activity was improved by a factor of 15 for Pd₃Ga₇ and a factor of 30 for PdGa by chemical etching. Given the low BET surface area of PdGa and Pd₃Ga₇ and a partial coverage of the surface by gallium oxide even after an optimized chemical etching, it appears that the activity per surface area, for instance, for etched PdGa is at least similar to that of Pd/Al₂O₃ (Table 3).

3.5. Increased Selectivity and Stability of PdGa and Pd₃Ga₇

The hydrogenation pathway from acetylene to ethylene and further to ethane (reactions 1-3) does not require assemblies of active sites in contrast to the oligomerisation reaction (4) leading to higher hydrocarbons [15,42,43]. Higher hydrocarbons can be dehydrogenated to form carbon deposits and, thus, deactivate the catalyst [44-49].



Di- σ -bonded acetylene and ethylene as well as vinylidene and ethylidyne species have been proposed as precursors for the acetylene oligomerisation. The main product of reaction 4 is 1,3-butadiene which can be further hydrogenated to 1-butene, n-butane, cis- and trans-butene (referred to as C₄-hydrocarbons). C₆- and higher hydrocarbons are also formed in small quantities.

In an excess of ethylene (gas composition B), ethane may be formed by total hydrogenation of adsorbed acetylene (reaction 3) or by adsorption and hydrogenation of ethylene from the gas phase (reaction 2). In the first case, a direct hydrogenation reaction path from acetylene to ethane [1,50-52] and a Horiuti-Polyani mechanism with consecutive addition of hydrogen [53,54] have been proposed. Because of the very low formation of ethane with gas composition A, a direct hydrogenation path from acetylene to ethane appears to play only a minor role on the surface of PdGa and Pd₃Ga₇ (Figure 3). Instead, the low ethane concentration and the formation of C₄ hydrocarbons indicate a preferred Horiuti-Polyani mechanism with consecutive addition of hydrogen. So, to obtain high selectivity in the semi-hydrogenation of acetylene in an excess of ethylene (gas composition B), minimizing the hydrogenation of ethylene (reaction 2) is most important.

The extremely high hydrogenation power of Pd – leading to unselective hydrogenation – is partly due to the

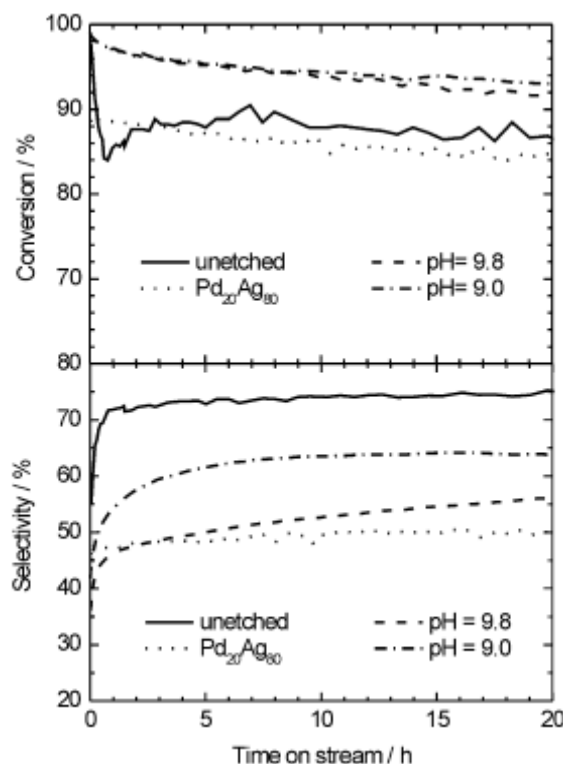


Figure 8: Conversion and selectivity of untreated PdGa (40 mg), PdGa chemically etched at pH 9.8 (1.5 mg) and pH 9.0 (5 mg) and Pd₂₀Ag₈₀ (200 mg) in acetylene hydrogenation (isothermal at 473 with gas composition B).

formation of β -palladium hydride and, thus, the presence of bulk-dissolved, very active hydrogen species [6,55-66]. Applying gas composition B to Pd/Al₂O₃ results in the hydrogenation of a significant part of ethylene from the feed and, correspondingly, in low selectivity. Interestingly, Pd can be switched to a selective catalyst, i.e. performing exclusively hydrogenation of alkynes to alkenes, by the formation of a sub-surface Pd-C phase which isolates the bulk dissolved, very active hydrogen from the surface [65,66]. However, the observed Pd-C phase is not stable in the absence of a hydrocarbon feed.

Aiming at the development of more stable and more selective catalysts the alloying of Pd with different metals, Ag [67], Sn [68], Au [69] or Ni [70] has been described. Industrial catalysts for the semi-hydrogenation of acetylene are based on Pd-Ag alloys with improved catalytic properties [7]. At high Ag/Pd ratio a partial isolation of Pd sites is achieved, decreasing the amount of oligomerisation products as well as ethane, thus increasing stability and selectivity (Pd₂₀Ag₈₀ in Figure 7). However, in disordered alloys one component tends to segregate to the surface, leading to either deactivation of the catalyst or loss of the selectivity by the formation of extended Pd active-sites. Furthermore, segregation of palladium goes hand in hand with the corresponding subsurface chemistry (e.g. the presence of hydrides). These effects are responsible for the only moderate selectivity of alloy systems.

The intermetallic compounds used in this study are a class of materials that can circumvent most of the listed

drawbacks. They are well ordered and exhibit localized, covalent interactions between Pd and Ga [10,34]. The coordination of the isolated Pd atoms is fixed by the crystal structure, while Pd-Ga interactions stabilize the structure and prevent sub-surface chemistry as well as hydride formation. These properties result in significantly higher selectivity and long-term stability of PdGa and Pd₃Ga₇ in the ethylene-rich feed of gas composition B (Figures 3 and 7, Table 3).

The reason for the absence of detectable CO chemisorption on PdGa and Pd₃Ga₇ at room temperature, besides the low surface area and the low Pd surface concentration, may be the modification of the electronic structure of the intermetallic compounds compared to palladium metal. Quantum-chemical *ab initio* calculations of the band structures and chemical bonding in PdGa and Pd₃Ga₇ (electron localization function ELF and electron localization indicator ELI) showed a significant contribution of covalent bonding which may account for the reduced adsorption energy of CO on the Pd sites of the intermetallic compounds [10,34].

PdGa exhibits a higher activity-per-mass ratio than Pd₃Ga₇. The higher activity can predominantly be assigned to the higher Pd content in PdGa (60.4 wt.-%) compared to Pd₃Ga₇ (39.5 wt.-%), which is also displayed in the Pd concentration of the surface (6% and 2%, respectively). Under the reaction conditions employed, untreated PdGa and Pd₃Ga₇ show a similar selectivity in acetylene hydrogenation. Conversely, chemical etching of Pd₃Ga₇ results in a more pronounced loss of selectivity compared to chemically etched PdGa. The decreased selectivity of chemically etched Pd₃Ga₇ may be caused by dissolution of Ga atoms from the bulk and preferred formation of ensembles of Pd atoms on the surface and is subject to more detailed research.

The combination of stable site-isolation, altered electronic structure and the absence of hydride formation makes PdGa and Pd₃Ga₇ ideally suited, selective and long-term stable hydrogenation catalysts. Further investigations, employing other well-characterized and unsupported palladium-containing intermetallic compounds, will help to understand the influence of the three effects on the selectivity and stability of catalysts in the semi-hydrogenation of acetylene.

4. Conclusions

In Part I of the work presented here, the particular structural properties of selected Pd-Ga intermetallic com-

pounds were described. *In situ* structural investigations of PdGa and Pd₃Ga₇ during thermal treatment in different gas atmospheres yielded a high structural stability without a detectable formation of hydrides or carbides. Moreover, as presented in Part II, PdGa and Pd₃Ga₇ possess superior catalytic properties in acetylene hydrogenation. Both intermetallic compounds exhibit a higher selectivity in acetylene hydrogenation than commercial supported Pd/Al₂O₃ and an unsupported Pd₂₀Ag₈₀ alloy. PdGa and Pd₃Ga₇ showed no deactivation during long-term acetylene hydrogenation compared to Pd/Al₂O₃.

The high selectivity and high stability can be assigned to the active-site isolation in the crystallographic structure of Pd-Ga intermetallic compounds which results in a “geometric effect”, leading to weakly π -bonded acetylene molecules on top of isolated Pd atoms, an “electronic effect” resulting in a modification of adsorption and desorption properties and a “kinetic effect” due to the decreased availability of hydrogen because of the absence of Pd hydrides.

“Active-site isolation” was the guiding concept of our knowledge-based investigation on improved acetylene hydrogenation catalysts. The successful application of structurally well-defined palladium containing intermetallic compounds confirms the value of a rational approach to catalyst development. The concept of using intermetallic compounds with at least partly covalent bonding interactions rather than alloys is a suitable way to arrive at long-term stable catalyst with pre-selected electronic and local structural properties.

Our concept yielded a material whose preparation, composition and structure would hardly have been obtained by any high-throughput screening in the periodic table of the elements. New preparation techniques and improved chemical treatment procedures will be pursued in the future and will yield high surface area materials with improved activity while maintaining high selectivity and stability in acetylene hydrogenation.

Acknowledgements

We thank J. Kröhnert and G. Tzolova-Müller for assistance with the CO chemisorption measurements. Collaboration and stimulating discussions with T. Ressler are greatly appreciated. We are grateful to the ATHENA cooperation partners for scientific discussion about palladium in heterogeneous catalysis and K.K. thanks the Max Planck Society for a research fellowship.

References

- [1] A.N.R. Bos, K.R. Westerterp, Chem. Eng. Process. 32 (1993) 1.
- [2] A. Borodzinski, G.C. Bond, Catal. Rev. 48 (2006) 91.
- [3] H. Arnold, F. Döbert, J. Gaube, in: G. Ertl, H. Knoerzinger, J. Weitkamp (Eds), Handbook of Heterogeneous Catalysis, VCH, Weinheim, 1997, p. 2165.
- [4] A. Molnar, A. Sarkany, M. Varga, J. Mol. Catal. A 173 (2001) 185.

- [5] P. Albers, J. Pietsch, S.F. Parker, J. Mol. Catal. A 173 (2001) 275.
- [6] B. Coq, F. Figueras, J. Mol. Catal. A: 173 (2001) 117.
- [7] M.M. Johnson, D.W. Walker, G.P. Nowack, US-Patent 4404124 (1983).
- [8] E.G. Derouane, J. Mol. Catal. 25 (1984) 51.
- [9] L. Guzzi, Catal. Today 101 (2005) 53.
- [10] K. Kovnir, M. Armbrüster, J. Osswald, T. Ressler, R.E. Jentoft, R. Giedigkeit, Yu. Grin, R. Schlögl, submitted to Angew. Chem. (2008).
- [11] E.W. Shin, C.H. Choi, K.S. Chang, Y.H. Na, S.H. Moon, Catal. Today 44 (1998) 137.
- [12] S. Leviness, V. Nair, A.H. Weiss, Z. Schay, L. Guzzi, J. Mol. Catal. 25 (1984) 131.
- [13] V. Ponec, Adv. Catal. 32 (1983) 149.
- [14] W. Palczewska, A. Jablonski, Z. Kaszukur, G. Zuba, J. Wernisch, J. Mol. Catal. 25 (1984) 307.
- [15] Y.M. Jin, A.K. Datye, E. Rightor, R. Gulotty, W. Waterman, M. Smith, M. Holbrook, J. Maj, J. Blackson, J. Catal. 203 (2001) 292.
- [16] J.H. Kang, E.W. Shin, W.J. Kim, J.D. Park, S.H. Moon, J. Catal. 208 (2002) 310.
- [17] V. Ponec, Applied Catal. A 222 (2001) 31.
- [18] E. Hellner, F. Laves, Z. Naturforsch. A 2 (1947) 177.
- [19] M.K. Bhargava, A.A. Gadalla, K. Schubert, J. Less-Common Met. 42 (1975) 76.
- [20] R. Giedigkeit, PhD thesis, Technische Universität Dresden, 2007.
- [21] H. Pfisterer, K. Schubert, Z. Metallkde. 41 (1950) 433
- [22] K. Khalaff, K. Schubert, J. Less-Common Met. 37 (1974) 129.
- [23] J. Osswald, R. Giedigkeit, R.E. Jentoft, M. Armbrüster, K. Kovnir, T. Ressler, Yu. Grin, R. Schlögl, European Patent 06005310.5 pending, 2006.
- [24] J. Osswald, R. Giedigkeit, R.E. Jentoft, M. Armbrüster, F. Girgsdies, K. Kovnir, T. Ressler, Yu. Grin, R. Schlögl, J. Catal. submitted (2008), part I of this study.
- [25] D. Briggs, M.P. Seah, Practical Surface Analysis by Auger and X-Ray Photoelectron Spectroscopy, Wiley, Chichester, 1988, p. 635.
- [26] J.W. Niemantsverdriet, Spectroscopy in Catalysis – an Introduction, Wiley-VCH, 2000, p. 79.
- [27] H. Dropsch, M. Baerns, Appl. Catal. A 158 (1997) 163.
- [28] H. Unterhalt, G. Rupprechter, H.J. Freund, J. Phys. Chem. B 106 (2002) 356.
- [29] J.J.F. Scholten, A. Vanmontfoort, J. Catal. 1 (1962) 85.
- [30] D.J.C. Yates, J.H. Sinfelt, J. Catal. 8 (1967) 348.
- [31] C. Sudhakar, M.A. Vannice, Appl. Catal. 14 (1985) 47.
- [32] M.B. Palmer, M.A. Vannice, J. Chem. Technol. Biotechnol. 30 (1980) 205.
- [33] G. Schön, J. Electron. Spectrosc. Relat. Phenom. 2 (1973) 75.
- [34] K. Kovnir, M. Armbrüster, D. Teschner, T. Venkov, F.C. Jentoft, A. Knop-Gericke, Yu. Grin, R. Schlögl, Sci. Technol. Adv. Mater. 8 (2007) 420.
- [35] K.I. Hadjiivanov, G.N. Vayssilov, Adv. Catal. 47 (2002), 307.
- [36] A.P. Seitsonen, Y.D. Kim, S. Schwegmann, H. Over, Surf. Sci. 468 (2000) 176.
- [37] C. Bryce, D. Berk, Ind. Eng. Chem. Res. 35 (1996) 4464.
- [38] [M.V. Lebedev, D. Ensling, R. Hunger, T. Mayer, W. Jaegermann, Appl. Surf. Sci. 229 (2004) 226.
- [39] C.C. Chang, P.H. Citrin, B. Schwartz, J. Vac. Sci. Technol. 14 (1977) 943.
- [40] K. Kovnir, J. Osswald, M. Armbrüster, D. Teschner, G. Weinberg, U. Wild, A. Knop-Gericke, T. Ressler, Yu. Grin, R. Schlögl, to be published.
- [41] K. Kovnir, J. Osswald, M. Armbrüster, R. Giedigkeit, T. Ressler, Yu. Grin, R. Schlögl. Stud. Surf. Science Catal. 162 (2006) 481.
- [42] N.A. Khan, S. Shaikhutdinov, H.J. Freund, Catal. Lett. 108 (2006) 159.
- [43] N.A. Khan, A. Uhl, S. Shaikhutdinov, H.J. Freund, Surf. Sci. 600 (2006) 1849.
- [44] S.K. Shaikhutdinov, M. Frank, M. Baumer, S.D. Jackson, R.J. Oldman, J.C. Hemminger, H.J. Freund, Catal. Lett. 80 (2002) 115.
- [45] N. Sheppard, C. De La Cruz, Vibrational Spectra of Hydrocarbons Adsorbed on Metals - Part II, Academic Press Inc, San Diego, 1998, p. 181.
- [46] G.C. Bond, Appl. Catal. A 149 (1997) 3.
- [47] E.M. Stuve, R.J. Madix, J. Phys. Chem. 89 (1985) 105.
- [48] S. Shaikhutdinov, M. Heemeier, M. Baumer, T. Lear, D. Lennon, R.J. Oldman, S.D. Jackson, H.J. Freund, J. Catalysis 200 (2001) 330.
- [49] H.J. Freund, M. Baumer, J. Libuda, T. Risse, G. Rupprechter, S. Shaikhutdinov, J. Catal. 216 (2003) 223.
- [50] J. Margitfalvi, L. Guzzi, A.H. Weiss, React. Kinet. Catal. Lett. 15 (1980) 475.
- [51] J. Margitfalvi, L. Guzzi, J. Catal. 72 (1981) 185.
- [52] J.M. Moses, A.H. Weiss, K. Matusek, L. Guzzi, J. Catal. 86 (1984) 417.
- [53] T.P. Beebe, J.T. Yates, J. Am. Chem. Soc. 108 (1986) 663.
- [54] P.A. Sheth, M. Neurock, C.M. Smith, J. Phys. Chem. B 107 (2003) 2009.
- [55] W. Palczewska, in: Z. Paal, P. G. Denon (Eds.), Hydrogen Effects In Catalysis, Marcel Decker, New York, 1988, p. 372.
- [56] G.C. Bond, P.B. Wells, J. Catal. 5 (1966) 65.
- [57] A.M. Doyle, S.K. Shaikhutdinov, S.D. Jackson, H.J. Freund, Angew. Chem. Int. Ed. 42 (2003) 5240.
- [58] A.S. McLeod, R. Blackwell, Chem. Eng. Sci. 59 (2004) 4715.
- [59] C.M. Pradier, M. Mazina, Y. Berthier, J. Oudar, J. Mol. Catal. 89 (1994) 211.
- [60] T. Komatsu, S. Hyodo, T. Yashima, J. Phys. Chem. B 101 (1997) 5565.
- [61] Q.W. Zhang, J. Li, X.X. Liu, Q.M. Zhu, Appl. Catal. A 197 (2000) 221.
- [62] M. Morkel, G. Rupprechter, H.J. Freund, Surf. Sci. 588 (2005) L209.
- [63] G. Rupprechter, G.A. Somorjai, Catal. Lett. 48 (1997) 17.
- [64] G. Rupprechter, M. Morkel, H.J. Freund, R. Hirschl, Surf. Sci. 554 (2004) 43.
- [65] D. Teschner, E. Vass, M. Havecker, S. Zafeiratos, P. Schnorch, H. Sauer, A. Knop-Gericke, R. Schlögl, M. Chamam, A. Wootsch, A.S. Canning, J.J. Gamman, S.D. Jackson, J. McGregor, L.F. Gladden, J. Catal. 242 (2006) 26.
- [66] D. Teschner, J. Borsodi, A. Wootsch, Zs. Révay, M. Hävecker, A. Knop-Gericke, S.D. Jackson, R. Schlögl, Science 320 (2008) 86.
- [67] D.C. Huang, K.H. Chang, W.F. Pong, P.K. Tseng, K.J. Hung, W.F. Huang, Catal. Lett. 53 (1998) 155.
- [68] S. Verdier, B. Didillon, S. Morin, D. Uzio, J. Catal. 218 (2003) 288.
- [69] T.V. Choudhary, C. Sivadinarayana, A.K. Datye, D. Kumar, D.W. Goodman, Catal. Lett. 86 (2003) 1.
- [70] P. Miegge, J.L. Rousset, B. Tardy, J. Massardier, J.C. Bertolini, J. Catal. 149 (1994) 404.

